Protactinium neutron-induced fission up to 200 MeV

V.M. Maslov
Joint Institute for Nuclear and Energy Research,220109, Minsk-Sosny, Belarus

Abstract

The theoretical evaluation of $^{230-233}$Pa(n,F) cross sections is supplemented by consistent description of fission probabilities, probed in transfer reactions. $^{230-234}$Pa fission probabilities and ratios of fission probabilities, surrogate for neutron-induced fission of respective target nuclides are analyzed in first-chance and emissive fission domains. First chance fission cross sections trends of Pa are based on consistent description of ^{232}Th(n,F), ^{232}Th(n,2n) and ^{238}U(n,F), ^{238}U(n,xn) data. The theoretical approach employed is supported by the ratio surrogate data by Burke et al., 2006, for the ^{237}U(n,F) reaction. Ratio surrogate data on the fission probabilities of ^{232}Th(^{6}Li,^{4}He)^{234}Pa and ^{232}Th(^{6}Li,d)^{236}U by Nayak et al.,2008, support the predicted ^{233}Pa(n, F) cross section at E_n=11.5-16.5 MeV. The predicted trends of ^{230,231,232}Pa(n, F) cross section up to E_n=20 MeV, are consistent with fissilities of Pa nuclides, extracted by statistical model analysis of ^{232}Th(p,F) (Isaev et al., 2008) and ^{232}Th(p,3n) (Morgenstern et al., 2008) data. The excitation energy and nucleon composition dependence of the transition from asymmetric to symmetric scission of fission observables of Pa nuclei is defined by analysis of p-induced fission of ^{232}Th at E_p=1-200 MeV. Predominantly symmetric fission in ^{232}Th(p,F) at $E_{n(p)}$=200 MeV as revealed by experimental branching ratios (Dujvestijn et al., 1999) is reproduced. Steep transition from asymmetric to symmetric fission with increase of nucleon incident energy is due to fission of neutron-deficient Pa (A≤229) nuclei. A structure of the potential energy surface (a drop of symmetric and asymmetric fission barriers difference ($E^f_{SYM} - E^f_{ASYM}$) from ∼3.5 MeV to ∼1 MeV) of N-deficient Pa nuclides (A≤226) and available phase space at outer fission saddles, are shown to be responsible for the sharp increase with $E_{n(p)}$ of the symmetric fission component contribution for ^{232}Th(p,F) and $^{230-233}$Pa(n,F) reactions. That is a strong evidence of emissive fission nature of moderately excited Pa nuclides, reliably quantified only up to $E_{n(p)}$ ∼20(30) MeV. Predicted fission cross section of ^{232}Pa(n,F) coincides with that of ^{232}Th(p,F) at $E_{n(p)}$>80 MeV, that means the entrance channel dependence of fission cross section with increase of nucleon incident energy diminishes. It is explained by later excitation of higher fissility Pa nuclides in p-induced fission reaction of ^{232}Th.

1 Introduction

Scarce neutron-induced fission measured database [1] for ^{231}Pa(n,F) and ^{233}Pa(n,F) was enriched recently by a few data sets [2, 3, 4], however they still do not cover the energy range of 0.001-20 MeV. Neutron-induced cross sections of ^{231}Pa(n,F) and ^{233}Pa(n,F)) data when complemented with a surrogate fission data, fission probabilities of $^{230-234}$Pa nuclides, measured in ^{232}Th(^{3}He,d)^{233}Pa, ^{231}Pa(d,p)^{232}Pa, ^{230}Th(^{3}He,d) ^{231}Pa and ^{230}Th(^{3}He,t)^{230}Pa at excitation energies 6-11.5 MeV [5] and fission probabilities of ^{232}Th(^{3}He,p)^{234}Pa and

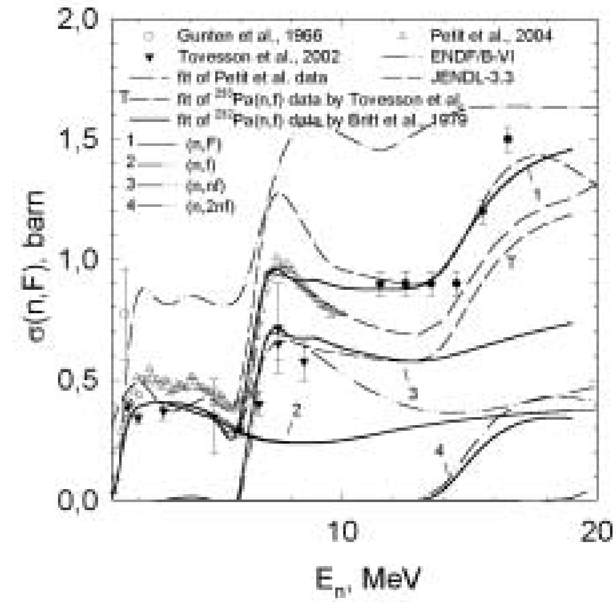

Figure 1: ^{233}Pa(n,F) reaction cross section.

^{232}Th(^{3}He,d)^{233}Pa, ^{232}Th(^{3}He,t)^{232}Pa at excitation energies 6-15 MeV [6] pose a number of severe problems for consistent theoretical description. In an emissive fission domain data by Petit et al. [6], as well as older indirect data by Birgul et al. [7] provoke assumption about steep decrease of the first-chance fission cross sections of ^{233}Pa(n,F) and ^{231}Pa(n,F) or/and systematically lowered fission probabilities of relevant Pa nuclides [8]. At excitations near fission threshold surrogate data [5, 6] are model-dependent via assumed neutron-absorption cross section and different angular momentum spectra of excited and fissioning states in neutron-induced and transfer fission reactions [9, 10]. At excitations higher than emissive fission threshold the sensitivity of the surrogate data to the angular momentum spectra of the nuclide fissioning in (n,nf) reaction may again increase. In particular case of even-even nuclide, fissioning via (n,nf) reaction, the cross section might be sensitive to the spectroscopic properties of collective states lying within a pairing gap. Another source of possible discrepancies might be pre-equilibrium effects, which are strongly pronounced in neutron-induced fission reactions, influencing first- and second-chance contributions. Recently developed surrogate ratio method [11] largely removes the uncertainty, imposed by pre-equilibrium effects and different angular momentum spectra of excited and fissioning states in neutron-induced and transfer reactions. The theoretical approach, which would be employed here for the $^{229-233}$Pa(n,F) cross section predictions, was independently supported by the ratio surrogate fissility data [11] for the ^{237}U(n,F) reaction [12, 13]. Recent ratio surrogate data on fission probability of ^{232}Th(^{6}Li,^{4}He)^{234}Pa and ^{232}Th(^{6}Li,d)^{236}U by Nayak et al. [14], relevant for the E_n = 11.5-16.5 MeV support our predicted ^{233}Pa(n,F) cross section [15, 16]. The shell effects either in fission fragments and saddle configurations define the fission observables at relatively low excitation energies. It is generally believed that with increase of the excitation energies the influence of the shell effects diminishes and fission observables should be dominated by the macroscopic nuclear properties. However, that simplified perception might be complicated by pre-fission neutron emission. It decreases the excitation energy of the fis-

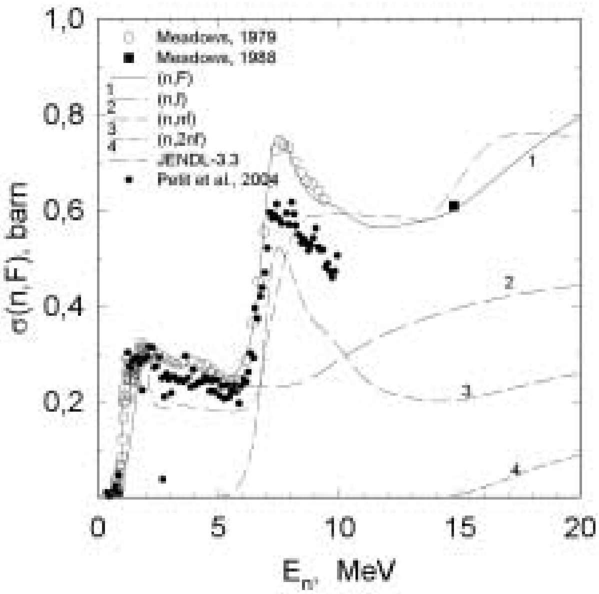

Figure 2: ^{230}Th(n,F) reaction cross section.

sioning nuclei, which may quite influence the competition of the symmetric and asymmetric fission modes [17, 18], decreasing the anticipated jump of the symmetric contribution. At the other hand, the neutron-deficient Pa nuclides, in ^{232}Th(p,$x$nf) or ^{232}Pa(n,$x$nf) reactions, might be more susceptible to symmetric fission even at low excitations [19, 20]. Interplay of these two trends would define the fission observables at higher excitations.

The striking difference of nucleon-induced fission cross sections of ^{232}Th target nuclide, i.e., those of ^{232}Th(p,F) and ^{232}Th(n,F) might be attributed to the influence of entrance channel and fissilities of Th and Pa nuclides. Fissilities of Pa nuclides could be fixed via ^{232}Th(p,F) cross section analysis. Comparison of ^{232}Th(p,F) and ^{232}Pa(n,F) would allow to infer the influence of entrance channel on the observed fission cross sections. That effect might be masked by the higher fissilities of neutron-deficient Pa nuclides, which are excited in ^{232}Pa(n,F) reaction at lower incident nucleon energies, than in case of ^{232}Th(p,F) reactions.

2 Direct/surrogate data for $^{230-233}$Pa(n,F) and ^{230}Th(n,F)

The surrogate data [6] are appreciably higher than direct ^{233}Pa(n,F) data [3, 4] both around ^{233}Pa(n,f) and second-chance ^{233}Pa(n,nf) fission thresholds (see Fig. 1). Similar discrepancies of direct and surrogate neutron-induced fission data were addressed by Arthur [21] in a combined analysis of the ^{235}U(n,f) data and ^{234}U(^{3}He,p)^{236}U reaction at $E_n \leq$3 MeV. It was observed [21], that when surrogate neutron-induced fission cross section is defined either as $\sigma_{nf} = \sigma_{CN} \times P_f^{exp}, \sigma_{CN}$ = 3.1 barn being the estimate of the neutron compound reaction cross section, or using optical model neutron absorption cross section as

$$\sigma_{nf} = \frac{\pi \acute{\lambda}^2}{2(2I+1)} \sum_{ljJ\pi} (2J+1) T_{lj}^{J\pi}(E_n) \times P_f^{exp}, \qquad (1)$$

the surrogate fission cross section overestimates σ_{nf} at $E_n \leq$2 MeV by 10-20%. That

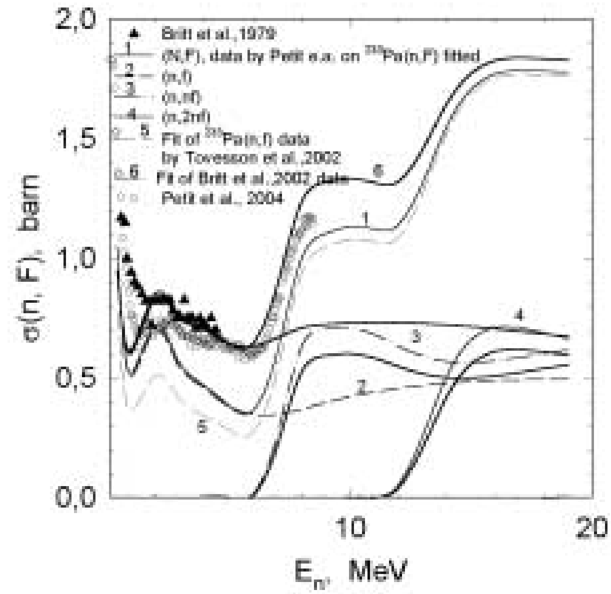

Figure 3: ^{232}Pa(n,F) reaction cross section.

is the consequence of the of the spin population differences in transfer and (n,f) reactions [21, 22]. In case when the observed fission probability data of transfer reactions

$$P_f^{exp} = \sum P_f^{J\pi}(U)\alpha^{J\pi}(U), \tag{2}$$

where $\alpha^{J\pi}(U)$ defines the spin populations, are fitted and $P_f^{J\pi}(U)$ are used in Eq. (1) instead of P_f^{exp}, the discrepancy of the neutron-induced cross section σ_{nf} data and surrogate data, diminishes [21, 22]. Much larger discrepancy is observed at the onset of the ^{233}Pa(n,nf) reaction, the σ_{nf} data being much lower (see Fig.1). In principle that discrepancy could be traced back to the oversimplified procedure of obtaining surrogate data as $\sigma_{nf} = \sigma_{CN} \times P_f^{exp}$ in the emissive fission domain, pre-equilibrium emission sensitivity and slight influence of spectroscopic properties of transition states of ^{233}Pa, fissioning in ^{233}Pa(n,nf) reaction. The latter effect for odd-even nuclide ^{233}Pa should be excluded, unlike the observed discrepancy of direct and surrogate ^{230}Th(^{4}He,^{3}He)^{231}Th data for ^{230}Th(n,F), which might be traced back to properties of even-even nuclide ^{230}Th, fissioning in ^{230}Th(n,nf) reaction (see Fig. 2).

The shape of the ^{230}Th(n,F) cross section at E_n = 6-9 MeV energy range is strongly controlled by the spectroscopic properties of the transition states of even-even ^{230}Th, fissioning in ^{230}Th(n,nf) reaction. Wide peak around E_n= 8 MeV, observed in [23, 24] (see Fig. 2) is described by lowering the negative parity octupole band of ^{230}Th due to mass-asymmetry of outer saddle deformations. The step-like irregularity at E_n=9 MeV was interpreted as being due to the excitation of two-quasi-particle states in the ^{230}Th at outer saddle deformations [25, 26]. It might be concluded that the discrepancy of surrogate [6] and direct fission data for ^{230}Th target nuclide above ^{230}Th(n,nf) fission threshold is of systematic character, possibly due to factorization of the fission probability and neutron absorption cross section to get surrogate neutron-induced fission cross section.

Above emissive fission threshold contributions to the observed fission cross section coming

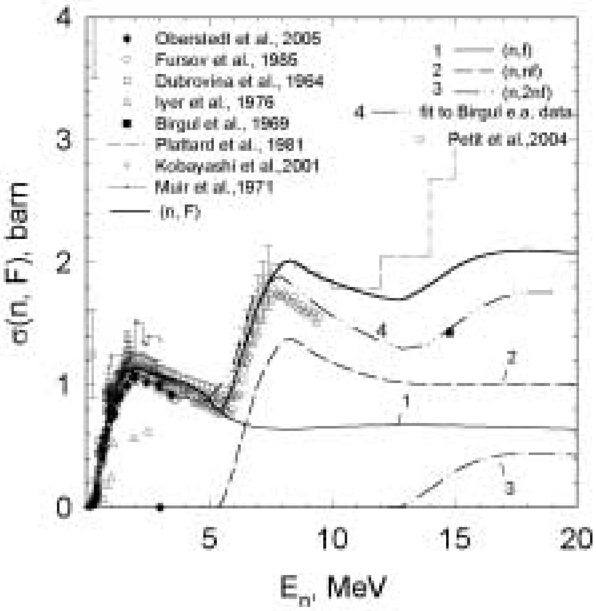

Figure 4: ^{231}Pa(n,F) reaction cross section.

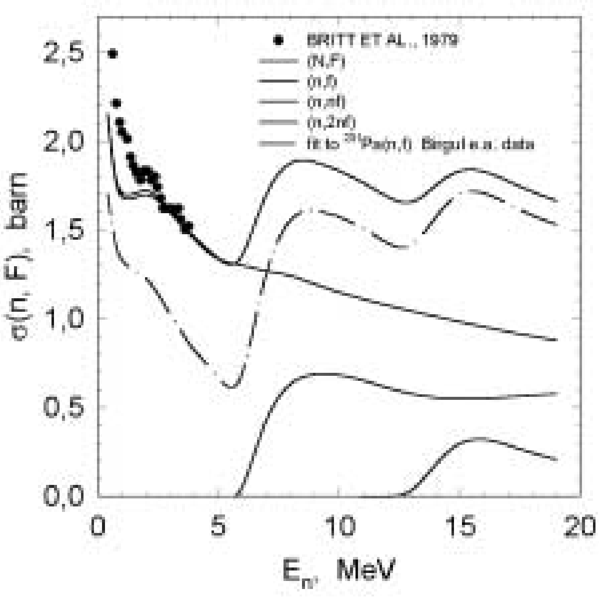

Figure 5: ^{230}Pa(n,F) reaction cross section.

from (n,$x$nf), $x = 1, 2, 3...X$, fission of relevant equilibrated uranium nuclei, is calculated as

$$\sigma_{nF}(E_n) = \sigma_{nf}(E_n) + \sum_{x=1}^{X} \sigma_{n,xnf}(E_n), \tag{3}$$

emissive fission contributions are calculated using fission probability estimates

$$\sigma_{n,xnf}(E_n) = \sum_{J\pi} \int_0^{U_{x+1}^{maax}} W_{x+1}^{J\pi}(U) P_{f(x+1)}^{J\pi}(U) dU, \tag{4}$$

where $W_{x+1}^{J\pi}$ is the population of $(x+1)$-th nucleus at excitation energy U after emission of x neutrons. Excitation energy U_{max} is defined by the incident neutron energy E_n and energy, removed from the composite system by ^{233}Pa(n,$x$nf) pre-fission neutrons. Fission probabilities of ^{233}Pa and ^{232}Pa nuclides, fissioning in ^{233}Pa(n,nf) and ^{233}Pa(n,2nf) reactions, respectively, are estimated using data of ^{232}Th(^{3}He,d)^{233}Pa [5, 6] and ^{231}Pa(d,p)^{232}Pa [6]. Overall consistency of ^{232}Th(^{3}He,d)^{233}Pa fissility data measured in [5, 6] is demonstrated on Fig. 3, showing neutron-induced fission cross section of ^{232}Pa(n,F). Calculated cross section was predicted in [15, 16] and confirmed by measured data of [6] up to $E_n \sim 7$ MeV, above which the discrepancy is similar to that, shown on Fig. 2, starts to occur (see Fig. 3).

Contribution of the first-chance fission to the observed fission cross section is defined by preequilibrium emission of first neutron and level densities of fissioning and residual Pa nuclides. The behavior of the first-chance fission cross section σ_{nf} is defined via first-chance fission probability P_{f1}as

$$\sigma_{nf} = \ \sigma_r(1 - q(E_n))P_{nf}. \tag{5}$$

The first neutron pre-equilibrium emission rate $q(E_n)$ is fixed by the consistent description of ^{238}U(n,F), ^{238}U(n,xn) and ^{232}Th(n,F), ^{232}Th(n,2n) data [27]. Fission barriers of Pa nuclei are believed to be three-humped, that is, the outer barrier has one more shallow well. The first-chance fission probability of the $^{230-234}$Pa nuclides in the emissive fission domain depends most strongly on the level density of fissioning and residual Pa nuclei. The ^{233}Pa(n,f) fission cross section shape, as predicted by the measured data [3, 4], could be fitted, but for that the contribution of the second chance fission reaction ^{233}Pa(n,nf) to the observed fission cross section of ^{233}Pa(n,F), should be extremely low. Consequently, calculated ^{232}Pa(n,f) cross section would be drastically discrepant with the surrogate data [5] on ^{232}Pa(n,f) at E_n ~0.5 -5 MeV (see Fig. 3). Above ^{233}Pa(n,nf) reaction threshold, data by Petit et al. [6] also could be fitted up to E_n ~10 MeV. Steep lowering of ^{233}Pa(n,F) cross section above E_n ~7 MeV is obtained by increasing the parameter value $\delta = \Delta_f - \Delta$, for ^{233}Pa fissioning nuclide from δ =0.075 MeV to δ=0.165 MeV, Δ_f and Δ are correlation function values at saddle and ground states. The former value of δ =0.07 MeV corresponds to the $\delta-$value for the ^{231}Pa fissioning nuclide (^{231}Pa(n,nf) fission reaction), which produces similar description of the ^{230}Pa(n,f) data by Britt and Wilhelmy [5] at $E_n \sim$ 2-5 MeV energy range. When fission probability of the ^{233}Pa is tuned to fit data by Petit et al. [6] above ^{233}Pa(n,nf) fission threshold, ^{232}Pa(n,f) cross section remains systematically lower than the surrogate data [5] at $E_n \sim$ 0.5 -5 MeV (see Fig. 3). However, shape of the ^{233}Pa(n,F) calculated cross section, obtained by fitting surrogate ^{232}Pa(n,f) data by Britt and Wilhelmy [5] in $E_n \sim$ 2-5 MeV energy range in [15, 16] is nicely supported by recent ratio surrogate data on the fission probabilities of ^{232}Th(^{6}Li,^{4}He)^{234}Pa and ^{232}Th(^{6}Li,d)^{236}U by Nayak et al. [14], relevant for the E_n ~11.5-16.5 MeV energy range. These surrogate data as well as ratio surrogate data [11, 28] are free of most strong systematic uncertainties of surrogate data, since only coincidences of fission and correlated particle are measured.

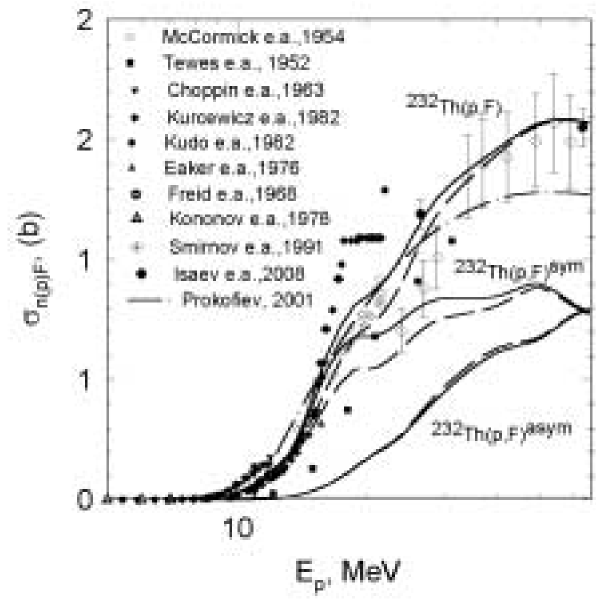

Figure 6: ^{232}Th(p,F) reaction cross section.

In case of ^{231}Pa(n,F) reaction (see Fig. 4) discrepancies of calculated cross section, based on direct data [29, 30, 31, 32, 33, 34], and surrogate data are quite similar to those, observed in case of ^{233}Pa(n,F). Data point by Birgul et al. [7] at $E_n \sim 14$ MeV is compatible with the trend, predicted by the surrogate data [6]. That trend and the data by Birgul et al.[7] could be reproduced if the contribution of the ^{231}Pa(n,nf) is much lower, than predicted by fission probability of the ^{231}Pa, defined from ^{230}Th(^{3}He,d)^{231}Pa reaction [5]. The first-chance fission cross section of ^{231}Pa(n,f) in the emissive fission domain has rather flat shape, as defined by the ratio of level densities of fissioning and residual Pa nuclei. The pre-equilibrium neutron contribution is fixed by major actinides data analysis.

Fig. 5 compares calculated cross sections of ^{230}Pa(n,F) with surrogate data [5]. Double-dot dashed curve shows the ^{230}Pa(n,F) fission cross section, decreased to fit the data point by Birgul et al. [7]. Fission probability for the nuclide ^{230}Pa, fissioning in ^{231}Pa(n,2nf) reaction, was estimated using fission probability data from the transfer reaction ^{230}Th(^{3}He,t)^{230}Pa [5]. The predicted trend of ^{231}Pa(n,F) cross section up to $E_n \sim$20 MeV, which is similar to that of ^{233}Pa(n,F), is consistent with fissilities of Pa nuclides, stemming from consistent analysis of ^{232}Th(p, F) and ^{232}Th(p,3n) data analysis.

The data base for p+^{232}Th interaction (for ^{232}Th(p,F):[35, 36, 37, 38, 39, 40, 41, 42], for ^{232}Th(p,3n): [39, 43, 44, 45, 46, 47] was enlarged by new data on ^{232}Th(p,F) [48] and ^{232}Th(p,3n) [49] for the excitation energy range, corresponding to $E_p \sim$15-30 MeV, where the fission probabilities of ^{231}Pa and ^{230}Pa are of major importance (see Fig. 6). Fit of ^{232}Th(p,F) and ^{232}Th(p,3n) (see Fig. 7) cross sections data corresponds to the present description of ^{231}Pa(n,F) cross section. Figure 6 shows, that the $E_p \sim$30 MeV contribution of symmetric fission mode to the observed fission cross section of ^{232}Th(p,F) reaction is rather low, however, at higher $E_p \gtrsim$80 MeV contribution of symmetric fission becomes larger, than

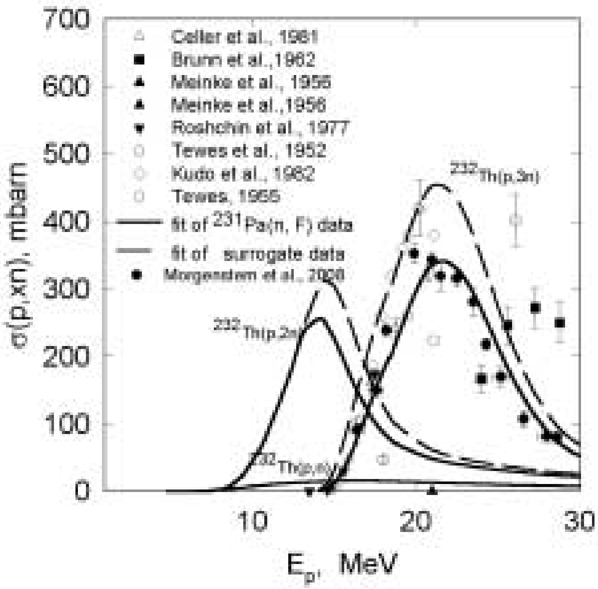

Figure 7: ^{232}Th(p,3n) reaction cross section.

that of asymmetric. In $^{230-233}$Pa(n,F) reaction cross section symmetric/asymmetric mode competition may be pronounced in different way. That may be attributed to influence of the entrance channel on the partial contributions of emissive fission reactions and to the respective observed fission cross sections, it will be demonstrated for ^{232}Th(p,$x$nf) and ^{232}Pa(n,$x$nf).

3 p+^{232}Th and n+$^{231-233}$Pa reactions

The excitation energy and (Z, N)-dependence of the transition from asymmetric to symmetric scission of fissioning Pa nuclei could be investigated for the ^{232}Th(p,F) reaction at $E_{n(p)}$=1-200 MeV energy range. That is the mass and excitation energy range, where the transition to predominantly symmetric fission was observed for the ^{232}Th(p,F) reaction [50, 51].

The data on the symmetric yield $r^{SL} = \sigma_{pF}^{SL}/(\sigma_{pF}^{SL}+\sigma_{pF}^{AS})$ for ^{232}Th(p,F) reaction of [50, 51, 53] probe incident proton energy range up to ∼200 MeV. Steep transition from asymmetric to symmetric fission for neutron-deficient Pa ($A \leq$229) nuclei (at excitations U ∼10 MeV) was predicted in [19]. For fission of ^{226}Th after fusion reaction (^{208}Pb(^{18}O,F)) still higher yield of symmetric fission component was observed at U ∼26 MeV [20]. At $E_{n(p)}$∼200 MeV about ∼20 neutron-deficient nuclides might contribute to the fission observables [26], while in [19, 20, 54] ν_{pre}=1-2. Symmetric/asymmetric (p(n),$x$nf) contributions to observed fission cross sections are largely defined by the level density parameters a_f and a_n for fissioning and residual nuclides, damping of the rotational modes contributions to the level densities and saddle asymmetries [26, 15, 55]. Distribution of the emissive fission chances ^{232}Th(p, xnf)/ ^{232}Th(p,F) at $E_{n(p)}$ =50 MeV peaks at x ∼3-4, at $E_{n(p)}$ =100 MeV it peaks are at x ∼6-8, at $E_{n(p)}$ =200 MeV the contributions of higher fission chances become overwhelming, peak shifts to x ∼17 for ^{232}Th(p,F) reaction [26, 56] (see Fig. 8).

The ^{232}Th(n,F) measured fission cross section data could be reproduced only for the fis-

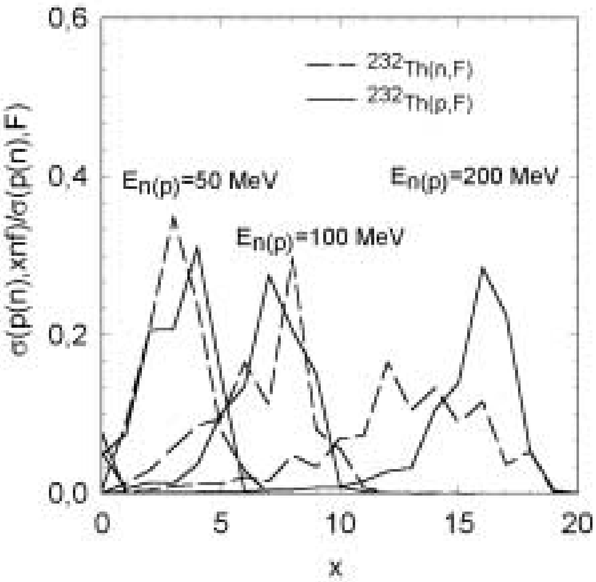

Figure 8: Emissive fission chances distribution of ^{232}Th(n,F) and ^{232}Th(p,F).

sion chances distribution, corresponding to the preferential contribution of fission of neutron deficient Th nuclides (see Fig. 9 and [26]). The data on ^{232}Th(p,F) and ^{232}Th(n,F) cross sections provide the complementary information on the evolution of the symmetric/asymmetric fission competition with increase of the projectile energy. The data on the ^{232}Th(p,F) (Fig. 9) observed fission cross section by Smirnov et al. [57] are supported by recent measurement by Isaev et al. [48]. The energy dependence of σ_{pF}^{SL} ($\sigma_{pF} = \sigma_{pF}^{SL} + \sigma_{pF}^{AS}$) is defined by the symmetry of the outer saddle of a double humped fission barrier. Present estimate of ^{232}Th(p,F) cross section differs essentially from the phenomenological estimate [58].

The measured symmetric fission yields for E_p= 20-50 MeV [53] and E_p= 190 MeV [50, 51] provide an unambiguous evidence for the sharp increase of r^{SL} at $E_p \geq$30 MeV (see Fig. 10). Observed ratio r^{SL} corresponds to different masses of fissioning Pa nuclei. The number of nuclides, making appreciable contribution to the observed symmetric fission cross section is lower than in case of asymmetric fission events. The reason for this is higher value of symmetric fission barrier. There is a strong evidence [19], that fission of $^{233-x}$Pa nuclei ($x =$ 1-20) in case of ^{232}Th(p,F) reaction would define competition of symmetric and asymmetric fission events at E_p up to 200 MeV. Partial branching ratios for ^{232}Th(p,f) and ^{232}Th(n, xnf) are shown on Fig. 10 as well. For lower fission chances r^{SL} reaches higher values at lower incident proton energies. For ^{232}Th(p,2nf) reaction maximum is attained at $E_p \sim 50$ MeV. Then it goes lower than r^{SL} for higher fission chances.

For ^{232}Th(n,F) it was found that rather thin but high axially asymmetric outer barrier (E_{fB}^{SL} corresponds to the mass symmetric fission, in contrary to the lower mass-asymmetric outer fission barrier (E_{fB}^{AS}). Similar barrier structure is assumed for the $^{215-234}$Pa nuclides. Sharing of the ^{232}Th(p,F) observed fission cross section to $SL-$ and $AS-$modes is compatible with the measured estimates of σ_{pF}^{SL} and σ_{pF}^{AS} [50, 51]. The estimate ($E_{fB}^{SL} - E_{fB}^{AS}$)=1.0 MeV is used for Pa nuclei with N $\leq$125. Figure 11 shows the $N-$dependence of ($E_{fB}^{SL} - E_{fB}^{AS}$) for pre-actinide nuclides, taken from symmetric/asymmetric fission yield analysis by Ohtsuki [60], and values for ^{230,232}Th nuclides, obtained in a microscopic Hartree-Fock plus BCS approach

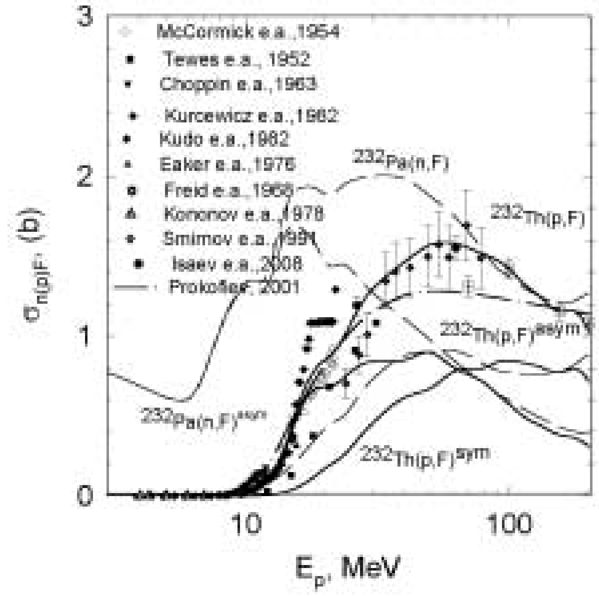

Figure 9: ^{232}Th(p,F) and ^{232}Pa(n,F) reaction cross sections.

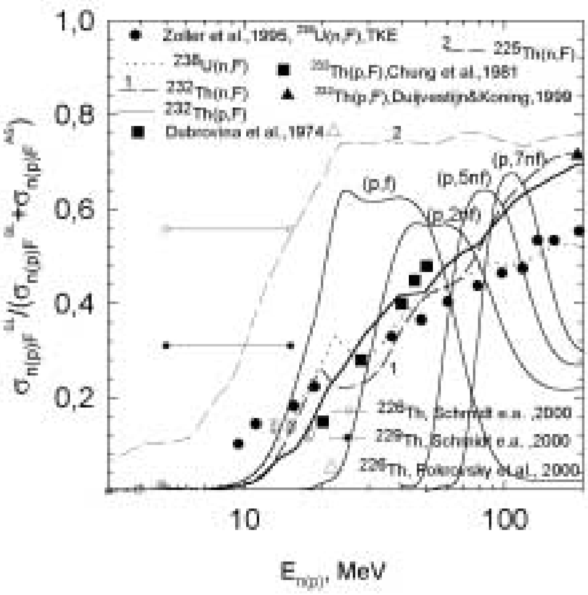

Figure 10: Ratio of symmetric to asymmetric fission events for ^{232}Th(p, F)and ^{232}Th(n, F)

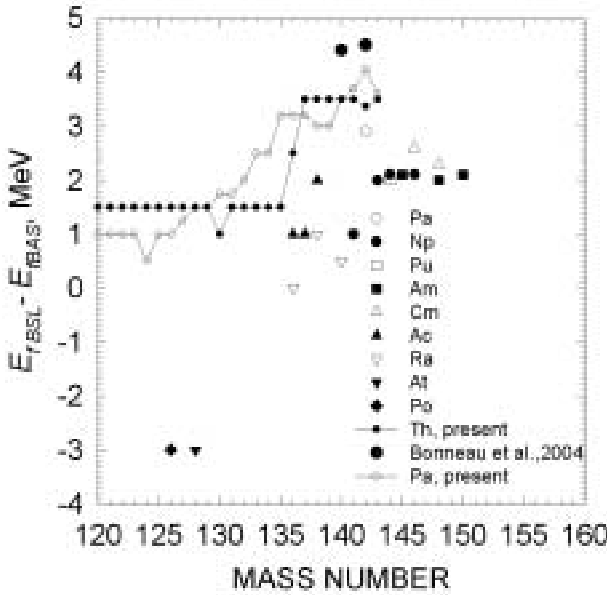

Figure 11: Fission barrier difference($E_{fB}^{SL} - E_{fB}^{AS}$) for symmetric and asymmetric outer saddles

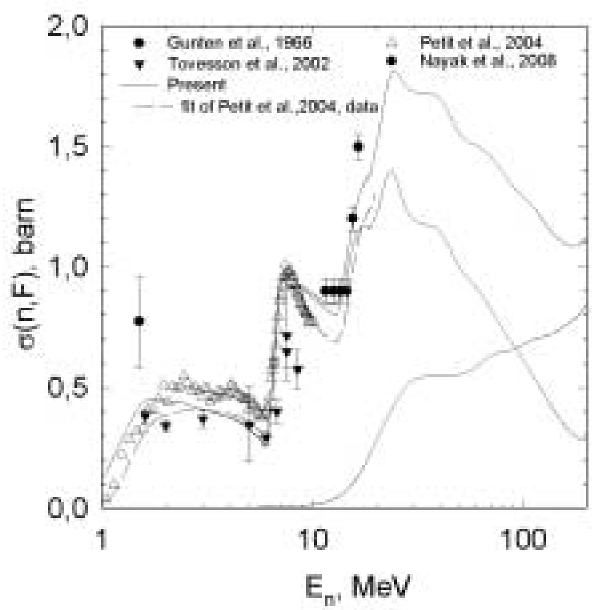

Figure 12: ^{233}Pa(n,F) reaction cross section.

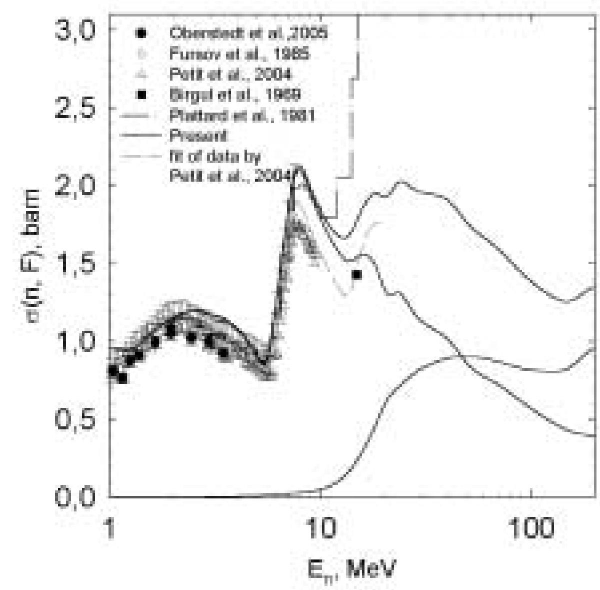

Figure 13: ^{231}Pa(n,F) reaction cross section.

by Bonneau et al. [61]. The $N-$dependences of $(E_{fB}^{SL} - E_{fB}^{AS})$ for Pa and Th nuclei, obtained in present approach, are not that strong as in case of Ra-Po nuclides, but still presents a challenge for the microscopic HFBCS calculations.

Prediction of the optical potential for the incident protons based on the optical potential for incident neutrons needs decomposition of the real and imaginary potential terms into isoscalar and isovector components [63]. For n+^{232}Th interaction we introduced isovector terms, which depend on the symmetry parameter $\eta = (N - Z)/A$, only in a real volume V_R^n and imaginary surface W_D^n potential terms [56, 59]. Values of V_R^p and W_D^p for incident protons could be calculated as $V_R^p = V_R^n + 2\alpha\gamma$ and $W_D^p = W_D^n + 2\beta\gamma$, $\alpha = 16$ and $\beta = 8$ values, obtained by the description of the proton and neutron scattering data for a number of medium weight nuclei [63, 64]. The predicted proton absorption cross section $\sigma_R^p > \sigma_R^n$ at $E_n \gtrsim$50 MeV is compatible with the experimental data in the same way, as it was shown for the p+^{238}U interaction [15].

Neutron-induced fission cross sections of $^{230-233}$Pa nuclides could be calculated with almost no free parameters, assuming the the pre-equilibrium contribution of first neutron emission for (n,nX) and (p,nX) reactions is fixed by consistent analysis of n+^{232}Th and p+^{232}Th interaction data. Figures 12 and 13 demonstrate fission cross sections of ^{233}Pa(n,F) and ^{231}Pa(n,F). Sharing of σ_{nF}^{SL} and σ_{nF}^{AS} is quite similar to that observed for ^{232}Th(n,F) reaction [26]. Proton-induced fission cross section of ^{232}Th is higher than that of neutron-induced fission of ^{232}Th at $E_{n(p)} \geq$18 MeV. That means in case of p+^{232}Th interaction the fissilities of Pa nuclei are relatively higher than those of respective Th nuclei for the n+^{232}Th interaction, which influences the observed fission cross section at $E_{n(p)}$ <100 MeV. In case of p+^{232}Th interaction entrance channel plays a decisive role at $E_{n(p)} \geq$100 MeV. The cross section of ^{232}Pa(n,F) reaction, shown on Fig. 9, is much larger than that of ^{232}Th(p,F) up to $E_{n(p)}$ ~80 MeV. At higher energies, though $\sigma_R^p > \sigma_R^n$,one observes $\sigma_{nF} \sim \sigma_{pF}$. That means entrance channel influence is compensated by the increase of the observed fission cross section of ^{232}Pa(n,F) due to earlier excitation of high fissility neutron-deficient Pa nuclides.

4 Conclusion

The evaluation of $^{230-233}$Pa(n,F) data up to E_n =200 MeV is based on consistent description of fission probability data, coming from transfer reactions and p+^{232}Th interaction data base. Recent ratio surrogate data on fission probabilities of ^{232}Th(^{6}Li,^{4}He)^{234}Pa by Nayak et al. [14] support the theoretical approach in case of ^{233}Pa(n,F) reaction. The predicted trend of ^{231}Pa(n,F) cross section up to E_n=20 MeV, which is similar to that of ^{233}Pa(n,F), is consistent with fissilities of Pa nuclides, stemming from analysis of ^{232}Th(p,F) and ^{232}Th(p,3n) data. The influence of the interplay of Pa fission barriers and entrance channel on the fission observables is shown to be different in case of n(p)+^{232}Th and n+^{232}Pa interactions. For p+^{232}Th and n+^{232}Th interactions the Pa nuclei are responsible for $\sigma_{pF} > \sigma_{nF}$ at 18≤$E_{n(p)}$≤100 MeV. Present estimate of ^{232}Th(p,F) cross section differs essentially from the phenomenological estimate [58]. For ^{232}Pa target σ_{nF} approaches σ_{pF} of ^{232}Th at $E_{n(p)}$∼80 MeV, remaining much larger at lower incident nucleon energies. The influence of the entrance channel seems to be compensated by excitation of higher fissility Pa nuclides in n+^{232}Pa interaction. In case of nucleon-induced fission of ^{232}Th the entrance channel plays a decisive role at $E_{n(p)}$ ≥100 MeV. The prediction of $^{231-233}$Pa fission cross sections up to E_n= 200 MeV was achieved for preferential contribution of fission of neutron-deficient nuclides. The measured data on symmetric fission yield for ^{232}Th(p,F) are reproduced, similar increase of symmetric fission yield for ^{231,232,233}Pa(n,F) reaction is predicted at E_n ∼50 MeV.

Support of International Science and Technology Center (Moscow) under the Project Agreement B-1604 is acknowledged.

References

[1] H.R. von Gunten, R.F. Buchanan, A. Wittenbach, Nucl. Sci. Eng. 27, 85 (1966).

[2] S. Oberstedt, S. Oberstedt, F-J. Hambsch et al., Ann. Nucl. Energy 32 (2005) 1867.

[3] F. Tovesson, A. Oberstedt, F-J. Hambsch et al., Phys. Rev. Lett. 88 (6), 062502-1(2002)

[4] F. Tovesson, F-J. Hambsch, A. Oberstedt et al., Nucl. Phys. A, 733, 3 (2004).

[5] H.C. Britt, J.B. Wilhelmy, Nucl. Sci. Eng., 72, 222 (1979).

[6] M. Petit, M. Aiche, G. Barreau et al., Nucl. Phys. A, 735, 3 (2004).

[7] O. Birgul, S.J.J. Lyle, Radiochimica Acta, 11, 108 (1969).

[8] G. Vladuca, F.-J. Hambsch, A. Tudora et al., Nucl. Phys. A 740 (2004)3.

[9] W. Younes and H.C. Britt, Phys. Rev. C 68, 034610 (2003).

[10] W. Younes and H.C. Britt, Phys. Rev. C 67, 024610 (2003).

[11] J.T. Burke, L.A. Bernstein, J. Escher et al., Phys. Rev. C 73 (2006) 054604.

[12] V.M. Maslov, Phys. Rev. C 72 (2005) 044607.

[13] V.M. Maslov Phys. Atom. Nucl., 71 (2008) 9.

[14] B.K. Nayak, A. Saxena, D.C. Biswas et al., Phys. Rev. C78, 061602(R) (2008).

[15] V.M. Maslov et al., Proc. of the International Conference on Nuclear Data for Science and Technology, September 26 - October 1, 2004, Santa Fe, USA, p. 354.

[16] V.M. Maslov, Proc. XII International Seminar on Interaction of Neutrons with Nuclei, Dubna, Russia, May 26-29, 2004, p. 332 (2004).

[17] A. Turkevich and J.B. Niday, Phys. Rev., 84 (1951) 52.

[18] U. Brosa et al., Physics Reports, 197 (1990) 167.

[19] K.-H. Schmidt et al., Nucl. Phys. A665 (2000) 221.

[20] M.G.Itkis, Yu. Ts. Oganesyan, G.G. Chubaryan et al., Proc. Workshop on Nucl. Fission and Fission-Product Spectr., Seissin, France, 1994, ed. by H. Faust and G. Fioni (ILL, Grenoble, 1994). p. 77.

[21] E.D. Arthur, Trans. Amer. Nucl. Soc. 1984 Annual Meeting,New Orleans, June 3-7, 1984, vol. 46, TNSAO 46, p. 759.

[22] J. Escher and F.S. Dietrich, Phys. Rev. C74 (2006) 054601.

[23] J.W. Meadows, in Proc. Int. Conf. on Nuclear Cross Sections for Technology, Knoxville, Tennessee, 22-26 Oct 1979, p. 479 (1979).

[24] J.W. Meadows, Journ. Ann. Nucl. Energy, 15 (1988) 421.

[25] V.M. Maslov, Nucl. Phys. A 743 (2004) 236.

[26] V.M. Maslov, Phys. Lett. B649 (2007) 376.

[27] V.M. Maslov et al., Phys. Rev. C 68, 034607 (2004).

[28] C. Plettner, H. Ai, C.W. Beausang et al., Phys. Rev. C **71**, 051602(R) (2005).

[29] B.I. Fursov et al., Atomnaya Energiya, 59 (4), 339 (1985).

[30] S. Plattard, G.F. Auchampaugh, H.W. Hill et al. Phys. Rev. Lett., 46, 633 (1981).

[31] Kobayashi K., Yamamoto S., Lee S. et al, Nucl. Sci.Eng., 139, 273 (2001).

[32] Muir D.W., Vesser L.R. Proc. conf. on Nucl. Cross Sections and Technology, March 1971, Knoxville. Washington, vol. 1, 292, (1975).

[33] Dubrovina S.M., Shigin V.A. J., DOK, 157, (3), 561(1964).

[34] Iyer R.H., Sampathkumar R., Chaudhuri N.K. P, BARC-872, 106 (1976).

[35] McCormick G.H., Cohen B.L., Phys. Rev. 96 (1954) 722.

[36] H.A. Tewes and R.A.James, Phys. Rev. 88 (1952) 860.

[37] G.R. Choppin, J.R. Meriwether and J.D. Fox, Phys. Rev. 131 (1963) 2149.

[38] W. Kurcewicz, J. Szerypo, P. Hornshoj et al., Zetchshrift Fyz. A. 305 (1982) 99.

[39] H. Kudo, H. Muramatsu, H. Nakahara et al. Phys. Rev. C 25 (1982) 3011.

[40] R.W. Eaker and G.R. Choppin. J. Inorg. Chem. 38 (1976) 31.

[41] Freid S.H., Anderson J.L., Choppin G.R., J. Inorg. Chem. 30 (1968) 3155.

[42] V.N. Kononov, E.D. Poletaev P.P. D'jachenko, Sov. J. Nucl. Phys. 27 (1978) 162.

[43] A.Celler, M. Luontama, J. Kantele, J. Zylich, Journ. Phys. Chem. 24 (1981) 930.

[44] C. Brunn, G.N. Simonoff, Phys. Rev., 23 (1962) 12.

[45] W.W. Meinke, G.C. Wick, G.T. Seaborg, Journ. Inorg. Chem. 3 (1956) 69.

[46] A. Tewes, Phys. Rev. 98 (1955) 29.

[47] A.Roshchin, S. Yavshits, V. Yakovlev et al., Phys.At. Nucl. 60 (1997) 1941.

[48] S. Isaev, R. Prieels,Th. Keutgen et al., Nucl. Phys. A809 (2008) 1.

[49] A. Morgenstern et al., Appl. Rad. and Isot., 66 (2008) 1275.

[50] M.C. Duijvestijn, A.J. Koning, J.P. Beijers et al., Phys. Rev. C 59 (1999) 776.

[51] M.C. Duijvestijn, A.J. Koning and F.-J. Hambsch, Phys. Rev. C 64 (2001) 014607.

[52] S.M. Dubrovina, V.I. Novgorodtzeva, L.N. Morozov et al., Sov. J. Nucl. Phys. 17 (1974) 240.

[53] C. Chung C. and J. Hogan, Phys. Rev. 24 (1981) 180.

[54] S.I. Mulgin, S.V. Zhdanov, N.A. Kondratiev et al., Nucl. Phys. A824 (2009) 1.

[55] V.M. Maslov, Nucl. Phys. A717 (2003) 3.

[56] V. M. Maslov, Nucl. Phys. A757 (2005) 390.

[57] A.N. Smirnov, I.Yu. Gorshkov, A.V. Prokofiev and V.P. Eismont, Proc. of XXI International Symp. On Nuclear Physics, November 408, 1991, Castle Gaussig, Germany, p. 214, World Scientific Publishing Co., Pvt., Ltd., Singapore, 1992.

[58] A.V. Prokofiev, Nucl. Instr. Meth. In Phys. Res., A463 (2001) 557.

[59] V.M. Maslov, Yu.V. Porodzinskij, N.A. Tetereva et al., Nucl.Phys. A736, (2004) 77.

[60] T. Ohtsuki et al., Phys. Rev. C 48 (1993) 1667.

[61] L. Bonneau et al., Eur. Phys. J. A 21 (2004) 391.

[62] V.M. Maslov, EuroPhysics Journal. A 21 (2004) 281.

[63] J.P. Delaroche, E.Bauge and P. Romain, In: Proc. International Conference on Nuclear Data for Science and Technology, Trieste, Italy, 1997, p. 206.

[64] P.G. Young , INDC(NDS)-335, p.109, 1994.